JOURNAL OF SOLID STATE CHEMISTRY 29, 237–251 (1979)

# The Effect of Reduction and Temperature on the Electronic Core Levels of Tungsten and Molybdenum in $WO_3$ and $W_xMo_{1-x}O_3$— A Photoelectron Spectroscopic Study

E. SALJE,* A. F. CARLEY, AND M. W. ROBERTS

*School of Chemistry, University of Bradford, Bradford, West Yorkshire, BD7 1DP, United Kingdom*

Received July 5, 1978; in revised form October 17, 1978

X-Ray photoelectron spectroscopy (XPS) has been applied to electrochromic, reduced $WO_3$ and $W_xMo_{1-x}O_3$ crystals. In metal-reduced phases containing crystallographic shear planes the formation of $Mo^{5+}$ (preferentially) and $W^{5+}$ is observed in addition to that of the six-valent states. $W^{5+}$ and $W^{6+}$ are also dominant in $H^+$-bombarded $WO_3$ indicating the formation of bronzes $H_xWO_3$. Significant differences are observed between single-crystal and "amorphous" oxides. The five-valent state is interpreted as being due to electron trapping and polaron formation. Under $Ar^+$ bombardment the crystallinity of the surface is destroyed and a continuous distribution of $W^0$, $W^{4+}$, $W^{5+}$, and $W^{6+}$ is found similar to that observed for amorphous thin films. At low temperatures the ($\varepsilon$–$\delta$) metal–insulator (M–I) transformation of $H^+$:$WO_3$ is accompanied by a spontaneous change in the linewidth of $W^{5+}$ core levels but not of $W^{6+}$ states. This is in accordance with recent theoretical approaches to M–I transformations.

## Introduction

It is commonly accepted that structural phase transformations are mainly created by processes such as instabilities of lattice vibrations, displacive transformations, or order–disorder phenomena. Additional effects due to instabilities of the electronic system are usually neglected because the coupling of electron wave functions with geometrical order parameters is assumed to be small. Although this assumption is correct for insulators with large gap energies and common metals it must be doubted for narrow band semiconductors, polaron materials, and all crystals showing metal—insulator (M–I) transitions. According to the fundamental work of Mott (*1, 2*), structural phase transitions may even occur on the basis of electronic delocalization in narrow band materials only.

The main reason for neglecting the electronic band structure mechanism in crystallography was the lack of an experimental method to determine electronic levels in single crystals. This situation has changed dramatically over the last 7 years when X-ray photoelectron spectroscopy (XPS) was developed and successfully used in surface chemistry. This technique provides knowledge of binding energies, including core and valence levels, of all atoms with a ca. 20-Å, thick surface layer. Thus a chemical analysis of this layer is possible. Furthermore, different valence states can be distinguished from chemical shifts of the electronic levels. It is therefore an excellent technique for studying surface reactions with gases (*3, 4*) or even solid-state reactions, and furthermore it gives information about the

* Permanent address: Mineralogisches Institut, TU Hannover, Welfengarten 1, West Germany.



0022-4596/79/080237-15$02.00/0

electronic density of states of the crystal. It therefore seemed very attractive to study the electronic properties of the best known electrochromic system $WO_3$–$MoO_3$ (*5, 6*). Both the structural and physical properties of the binary oxides have been widely examined and very recently the series of mixed crystals $W_xMo_{1-x}O_3$ has been synthesized and investigated (*7*). It was found that at least 18 structural phase transitions take place, one of which is correlated with an M–I transformation ($\varepsilon$–$\delta$). In the low-temperature $\varepsilon$-phase conductivity occurs according to a hopping mechanism and optical absorption measurements on slightly $H^0$-doped material reveal a strong electron–phonon coupling which was interpreted in terms of small polaron formation (*8*). During the structural transformation from the monoclinic ($z = 4$) low-temperature phase to the triclinic ($z = 8$) room-temperature modification, the electronic properties of the crystal are fundamentally changed. From measurements of the Hall and Seebeck constants by Berak and Sienko (*9*) we know that the charge carrier density in $WO_3$ increases by a factor of 230 in the room-temperature phase. At room temperature, the conductivity is explained by rather tightly bound ($\alpha = 3$) large polarons. The same authors found that in slightly reduced $WO_{3-x}$ ($x \leq 0.0002$) the charge carrier density increased with the loss of oxygen, each removed oxygen ion releasing two free electrons into the crystal. In more reduced material ($x \leq 0.001$) most of the electrons (ca. 75%) are trapped and do not contribute to conductivity.

The enormous coupling between the charge density and the structural phase transition is clearly brought out by the fact that an increase in the number of free electrons shifts the phase-transition temperature to lower values ($-27$°C for $n = 2.10^{18}$ cm$^{-3}$ in contrast to $-46$°C for $n = 20.10^{18}$ cm$^{-3}$) and even destroys the stability of the low-temperature phase for highly reduced material (e.g., $WO_{2.9}$).

Much attention has recently been given to the phenomenon of electrochromism in these compounds. Electrochromism basically consists of the possibility of changing the colour of a crystal under the influence of an external electric field. The colour remains after the exciting field has been removed but the crystal can be bleached again by reversing the field. Materials showing electrochromism can be used as optical displays. According to Schirmer *et al.* (*10*) the application of $WO_3$ as an electrochromic device is restricted to amorphous films due to the small polaron formation in amorphous material. However single crystals can easily be coloured using the electrolytic method given by Hoppmann and Salje (*11*). The virgin $WO_3$ crystal shows a yellowish colour which is converted to deep blue-black under the influence of the electric field. This colour is similar to the appearance of the reduced oxides and nonmetallic sodium tungsten bronzes.

To understand this phenomenon, two principle questions arise: (i) How are charge carriers trapped in these compounds?, and (ii) what is the influence of the crystal structure on this process?

Previous XPS work on amorphous $WO_3$ (*12*) and fine powders (*13a,b*) shows that photoelectron spectroscopy can distinguish between reduced and unreduced tungsten positions. Although these studies suffer from the lack of structually well-defined surfaces, their comparison with results on crystalline materials should elucidate the influence of crystal structure on electronic energy levels.

## Experimental Approach

X-Ray photoelectron spectroscopy (XPS) has progressed from the pioneering work of Siegbahn and co-workers (*14*) so that it is now used in almost a routine way to study the nature of solids and their surfaces. The technique consists briefly of irradiating a sample with X rays of a particular energy $h\nu$

and energy analyzing the photoemitted electrons. The kinetic energy of an emitted electron $E_k$ is given by Eq. (1):

$$E_k = h\nu - (E_i - E_f), \quad (1)$$

where $E_f$ is the energy of the final state (of the singly ionized system) and $E_i$ is the energy of the initial state (of the neutral system). The binding energy $E_B$ of the electron is simply

$$E_B = E_i - E_f \quad (2)$$

and is usually equated with the energy of the corresponding level in the neutral atom via the frozen orbital approximation (Koopmans' theorem) which ignores relaxation of the other electrons in the atom or solid during the photoemission process. Since the energy levels in the neutral system are quantized, the photoelectron spectrum consists basically of discrete peaks, superimposed on a background due to the electrons which have been inelastically scattered in the solid before reaching the detector. A chemical analysis of the sample is thus possible. Final-state effects such as spin–orbit and spin–spin interactions and electron shake-up and shake-off processes result in additional spectral features (*15*). Coupling between the corehole and valence electrons may give rise to an asymmetrical broadening of the observed core-level spectra (*16a, b*).

In practice $E_B$ is usually referred to the Fermi level of the spectrometer,

$$E_B = h\nu - E_k - \phi_{sp}, \quad (3)$$

where $\phi_{sp}$ is the work function of the spectrometer. Determination of $\phi_{sp}$ is not straightforward, and spectral positions are therefore calibrated with respect to a peak of accurately known binding energy. The calibrant is generally either the C (1*s*) level from the contamination layer found on most samples or the core level of a metal (usually gold) evaporated *in situ* onto the sample surface. This procedure compensates for possible shifts in the measured $E_k$ due to buildup of charge on poorly conducting samples. An additional shift in the observed $E_B$ may arise from changes in the Fermi level of the sample (which need not be the same as the Fermi level of the spectrometer). These two effects are clearly not important for metallic samples. Relaxation energy shifts may also complicate interpretation of experimental binding energies. A review of the problems encountered in the calibration of photoelectron spectra has recently been given by Evans (*18*).

There are two principal features of the XPS technique:

(a) The binding energy of a core-level electron in an atom is sensitive to the local electron density (and therefore to the nature of the bond between it and surrounding atoms) giving rise to the so-called "chemical shift" in $E_B$. It is thus possible, in principle, to observe for example changes in the valence state of a particular species, subject to the considerations mentioned above. Qualitatively, chemical shifts have been correlated with changes in the effective charge localized on the atom, a decreasing negative charge resulting in an increase in $E_B$.

(b) The method is surface sensitive. Mean free paths for inelastic scattering of photoelectrons of ca. 1000 eV kinetic energy are of the order of 1.5 nm in most solids, so that information contained in X-ray photoelectron spectra relates predominantly to the outer few atomic layers. The surface sensitivity may be enhanced by reducing the electron take-off angle (angle between emitted electrons and the surface plane). Should the properties of this surface region differ markedly from those of the bulk then this will clearly be a disadvantage for those interested in the volume properties of the sample.

The two spectrometers used in this study have been previously described (*17a, b*). The pressure in the spectrometer is typically $<2 \times 10^{-7}$ Pa. The sample holder has an area of ca. 2 $cm^2$, although crystals as small as ca. 5 $cm^2$ may be examined. Both the Mg$K\alpha_{1,2}$($h\nu$ = 1253.6 eV) and the Al$K\alpha_{1,2}$($h\nu$ =

1486.6 eV) characteristic X-ray lines have been used in this investigation. *In situ* sample treatments available are bombardment by $Ar^+$ or $H^+$ ions using an ion gun, evaporation of calibrant metal films, and heating or cooling of the sample in the temperature range 77 to 900°K.

## Preparation of the Samples

Three different types of crystals have been examined: single crystals of $WO_3$, coarse grains of mixed crystals $W_{0.53}Mo_{0.47}O_3$, and reduced crystals $(W, Mo)O_{2.9}$. The single crystals of $WO_3$ were prepared by sublimation at 1420°C (*19*). The area of the crystal used for XPS was ca. 4 $mm^2$, the thickness 1 mm. The colour of this multi-twin crystal was yellowish green. Although deeper colours of tungsten oxides often mean a slight reduction of the crystal, a careful electron microscopic study of a small piece of this crystal revealed no lattice faults such as crystallographic shear planes, and no reduced tungsten states have been found in subsequent XPS examinations. Furthermore, optical absorption experiments in the near infrared region, which are extremely sensitive to substoichiometry (*9*), showed no oxygen loss whatsoever. The crystal is therefore assumed to be fully oxidized $WO_3$. The crystal was cleaved along (001) just before the experiment and immediately brought into the vacuum chamber.

The preparation of the mixed crystals $W_xMo_{1-x}O_3$ is described by Salje *et al.* (*7*). The crystal grains used in these experiments were enclosed in glass ampoules after the crystal growth and not exposed to air until the beginning of the experiment. The colour of the sample used is bright yellow and the average grain size is approximately 0.1 mm. To ensure good electrical contact between the crystals and the specimen holder the crystals were pressed into a thin Al foil which was then screwed onto the holder. The same procedure was also used for the reduced crystals. Following the method of Engstroem *et al.* (*20*), $WO_{0.53}Mo_{0.47}O_3$ was thoroughly mixed with tungsten metal and heated to 570°C in sealed silica tubes. The black reaction product $[W, Mo]O_{2.9}$ was first examined electron microscopically. It showed arrays of crystallographic shear (*CS*) planes in the direction (102) with an average superstructure of $n = 14$, but no macroscopic segregation of W and Mo. The same crystals were used by Engstroem, *et al.* (*20*) to determine the phase diagram of the reduced oxides. The tungsten–molybdenum ratio of the reduced crystals was determined from the XPS data.

## Experimental Results

### (*a*) *Chemical Analysis*

To determine the chemical composition of the crystals, full-scan spectra were taken. They are shown in Fig. 1 for pure $WO_3$ and $W_{0.53}Mo_{0.47}O_3$ together with the indexing of the core levels. Both spectra show, beside the elements W, Mo, and O, small amounts of C (contamination) and Al and Au from the specimen holder. They are well separated from the W, Mo, and O peaks and do not affect the interpretation of the XPS spectra. In pure $WO_3$, the intensity ratio $W^{4+}/O\ 1s = 0.91$ is estimated from XPS peak heights. In $W_{0.53}Mo_{0.47}O_3$ this ratio is reduced by ca. 50% compared with $WO_3$, in good agreement with that anticipated from the chemical formula. Similarly, the reduced ternary oxide was shown to have the composition $W_{0.8}Mo_{0.2}O_{2.9}$.

### (*b*) *Reduction and Chemical Shift*

The fine structure of the tungsten $4f$ and the molybdenum $3d$ levels in Figs. 2 and 3 shows considerable changes after reduction of the crystals. In fully oxidized compounds only two levels ($4f_{7/2}$ and $4f_{5/2}$ in W and $3d_{5/2}$ and $3d_{3/2}$ in Mo) appear. In the reduced crystals, the superimposition of two doublets induces more broadened features

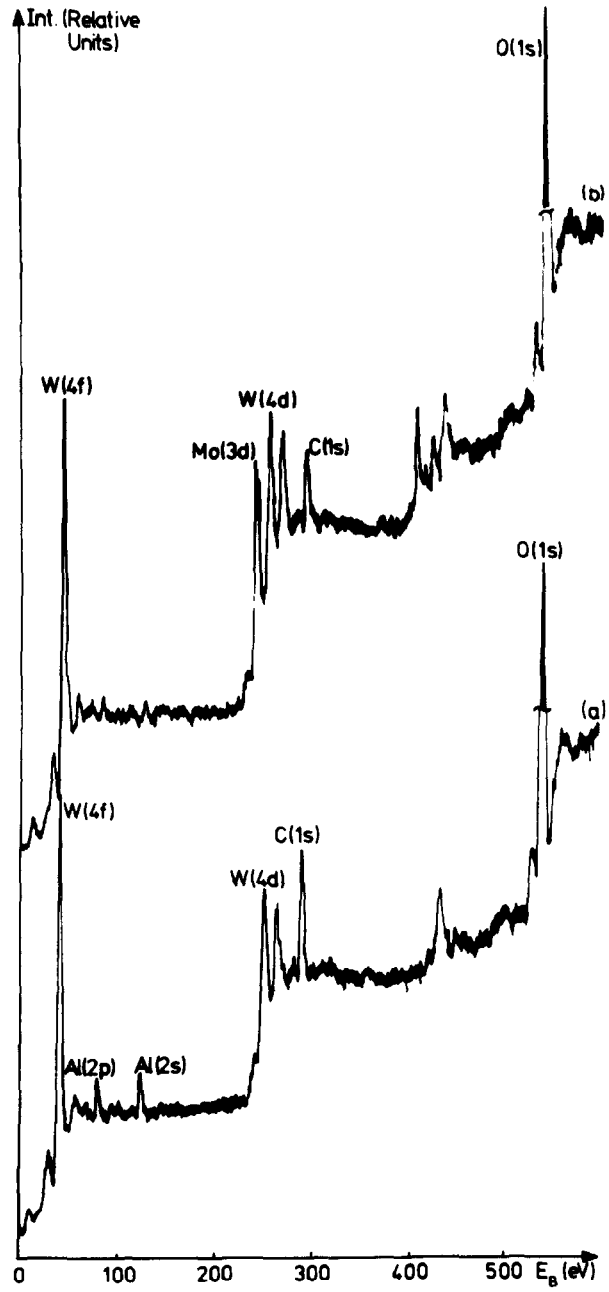


FIG. 1. Wide-scan X-ray photoelectron spectra for: (a) unreduced $WO_3$, (b) unreduced $W_{0.53}Mo_{0.47}O_3$.

[as also observed by de Angelis and Schiavello (*13b*) for nonstoichiometric tungsten oxides]. In tungsten and molybdenum the shifts during reductions $W^{6+} \rightarrow W^{5+}$ and $Mo^{6+} \rightarrow Mo^{5+}$ are revealed by a curve-fitting procedure (*21*) as given in Table I. In addition to these peaks, in unreduced crystals a further small feature appears at a binding energy ca. 6 eV higher than that of the W 4*f* doublet. The nature of this satellite has been

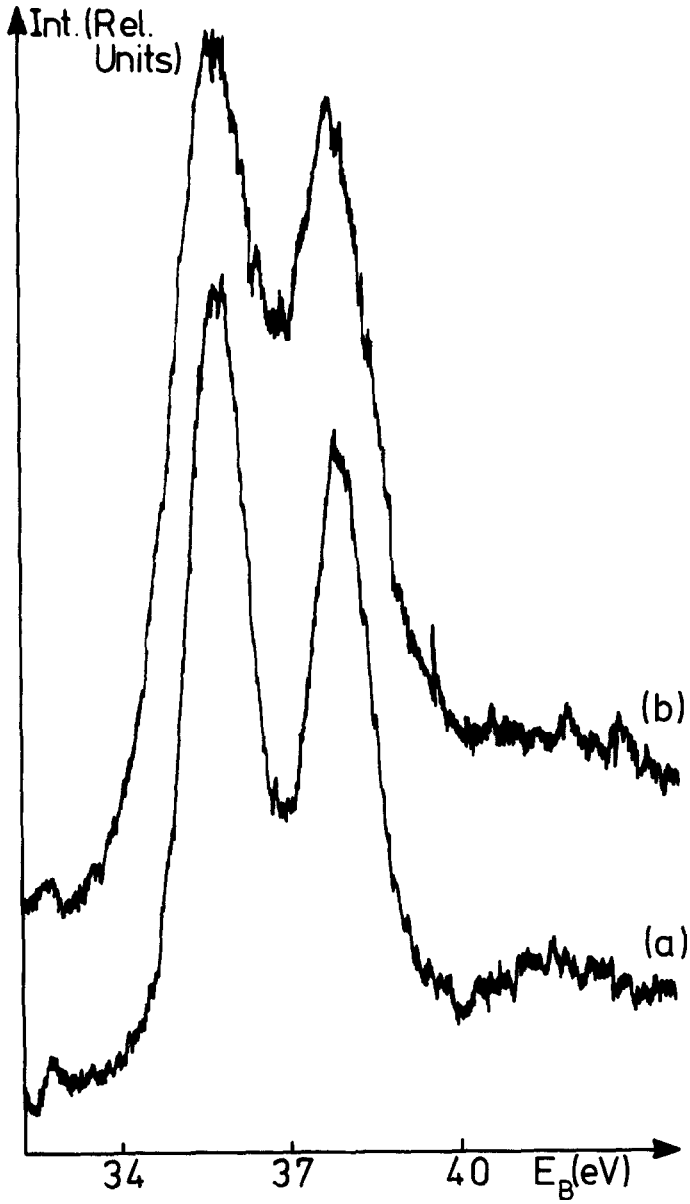


FIG. 2. W(4*f*) spectral region for $WO_3$: (a) unreduced crystals, (b) reduced crystals.

discussed by several workers (*22, 23, 38*). During our experiments with crystals we found very little, if any, reduction of the samples due to X-ray bombardment.

(*c*) *Ion bombardment*

Reduction of the fully oxidized material was achieved by ion bombardment. Two different types of experiment were performed using $H^+$ and $Ar^+$ ions. The XPS data obtained after $H^+$ bombardment are shown in figs. 4 and 5. For a hydrogen partial pressure of $10^{-6}$ Torr and an acceleration voltage of 400 V the principal features of the spectra are identical to those of reduced $WO_{2.9}$. The W4*f* peaks consist of $W^{6+}$ and $W^{5+}$ with the

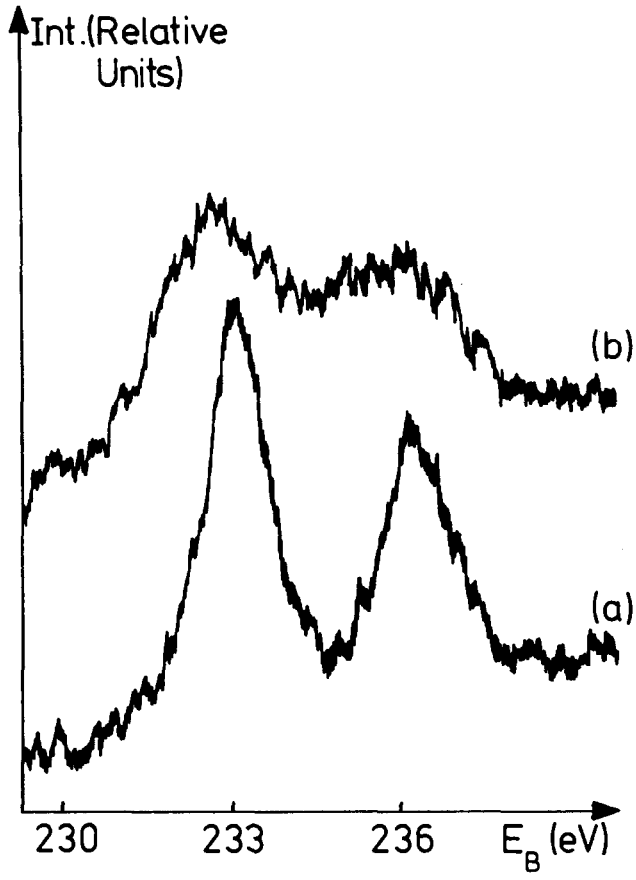


FIG. 3. Mo($3d$) spectral region for $MoO_3$: (a) unreduced crystals, (b) reduced crystals.

TABLE I

CURVE-FITTING DATA FOR $W^{6+}$, $W^{5+}$, $Mo^{6+}$, AND $Mo^{5+}$ [a]

| Ion | Ratio 5+/6+ | $\Delta(6+-5+)$ [b] (eV) | Full width at half-maximum (eV) | |
|---|---|---|---|---|
| | | | 6+ | 5+ |
| W in $WO_3$ | 0 | — | 1.35 | — |
| W in $W_{0.53}Mo_{0.47}O_3$ | 0 | — | 1.35 | — |
| Mo in $W_{0.53}Mo_{0.47}O_3$ | 0 | — | 1.45 | — |
| W in $W_{0.8}Mo_{0.2}O_{2.9}$ | 1.3 | ~1 | 1.70 | 1.45 |
| Mo in $W_{0.8}Mo_{0.2}O_{2.9}$ | 20.0 | 1.1 | 2.4 | 1.8 |
| W in $H^+$:$WO_3$ (300°K) | 19.0 | 1.2 | 1.70 | 1.45 |
| W in $H^+$:$WO_3$ (300°K) | 9.3 | 1.3 | 1.70 | 1.50 |
| W in $H^+$:$WO_3$ (77°K) | 6.8 | 1.3 | 1.70 | 1.10 |

[a] Binding energies: $W^{6+}$ ($4f_{7/2}$) = 35.7 eV, $Mo^{6+}$ ($3d_{5/2}$) = 233.1 eV.
[b] Shift between 6+ and 5+ binding energies.

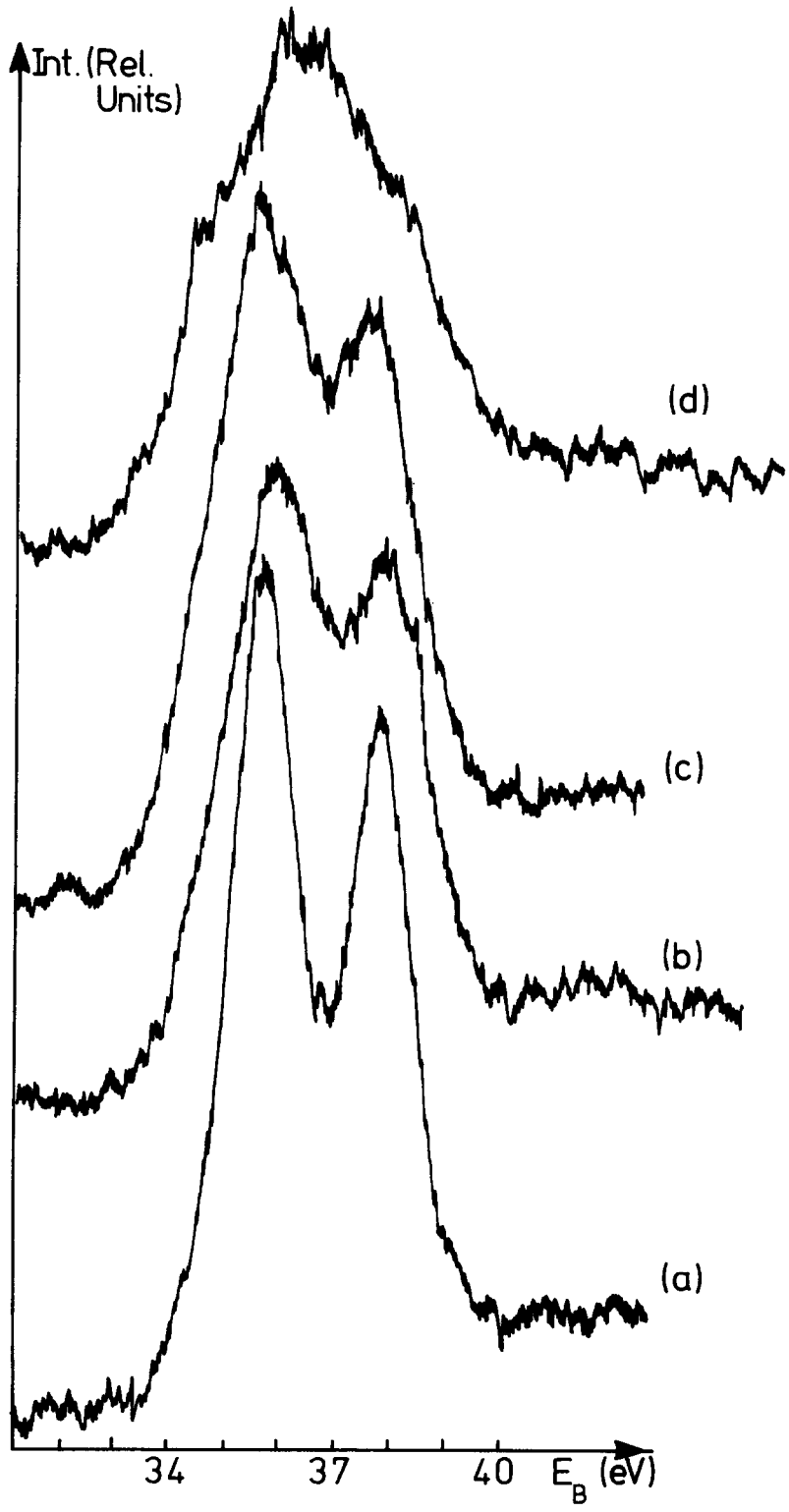


FIG. 4. W(4*f*) spectra from $WO_3$: (a) for as-prepared crystals, and after hydrogen ion bombardment (hydrogen pressure = $10^{-6}$ Torr, accelerating potential = 400 V, sample temperature = 300°K) for (b) 30 min., (c) 45 min., and (d) 11 hr.

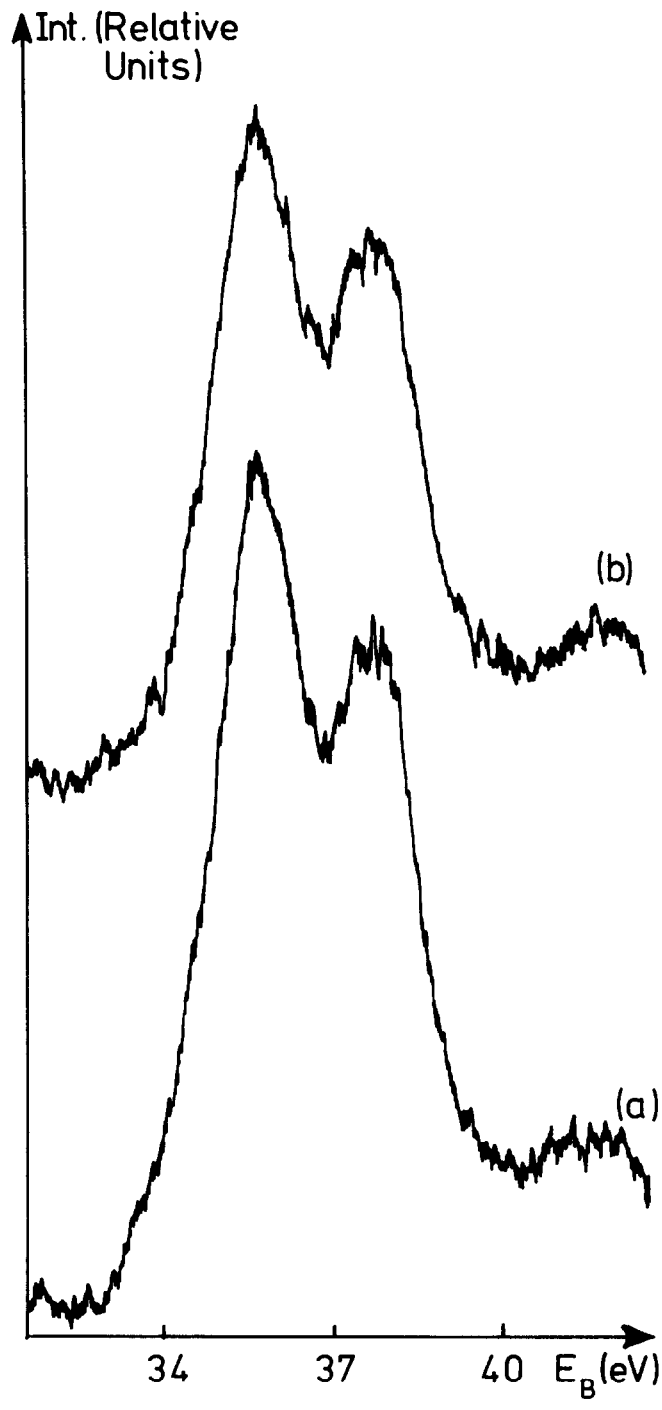


FIG. 5. W(4*f*) spectra from $WO_3$: (a) after hydrogen ion bombardment (hydrogen pressure = $10^{-6}$ Torr, accelerating potential = 400 V, sample temperature = 300°K) for 80 min., and (b) after cooling the bombarded sample to 77°K.

ratio $W^{5+}/W^{6+}$ depending on bombarding time according to Fig. 6. In the early stages of reduction an exponential increase in the $W^{5+}/W^{6+}$ ratio with time is observed. After 1 hr of bombardment this ratio saturates at ca. 25%, which is close to the critical value of the structural phase transformation between semiconducting and metallic tungsten bronzes. It appears that higher degrees of reduction together with the formation of pseudocubic, metallic $H_xWO_3$ are difficult to achieve under these (low pressure) conditions. After prolonged reduction (20 hr) only small changes in the tungsten states appear from the single-crystal spectra. At any stage, a subsequent heating of the crystal *in vacuo* at 220°C diminished the concentration of $W^{5+}$. The reduction of $WO_3$ under $H^+$ bombardment therefore appears to be, at least partly, reversible, in that hydrogen is removed from the surface region of the crystal under these conditions. This result is in accordance with the observed reversibility of electrolytically reduced tungsten oxide (*11*).

However, under bombardment with hydrogen at a higher pressure ($5 \times 10^{-5}$ Torr), further features in the W4*f* signals appear. A curve fitting of the XPS data using only two doublets shows the dominance of the $W^{5+}$ state together with an anomalous increase in the half-width of this peak to 2.25 eV (compare Table I). This indicates that further reduced states like $W^{4+}$

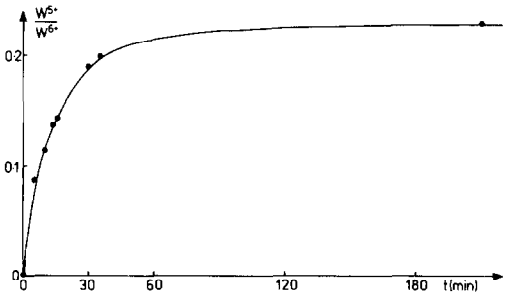


FIG. 6. Plot showing the variation of the $W^{5+}$:$W^{6+}$ ratio with hydrogen ion bombardment time (hydrogen pressure = $10^{-6}$ Torr, accelerating potential = 400 V, sample temperature = 300°K) for a $WO_3$ sample.

have been created, which are reversible upon heating the crystal *in vacuo*. These single-crystal data are different from the spectra observed by Haber *et al.* (*13a*) with powder samples. In all the spectra obtained with single crystals the $W^{6+}$ and $W^{5+}$ states are dominant and only after extended hydrogen bombardment do the $W^{4+}$ peaks appear.

In contrast to the small protons the large $Ar^+$ ions usually destroy the crystallinity of surfaces and reduce oxides by mechanically removing oxygen from the crystal. In Fig. 7 the results of the $Ar^+$ bombardment at $10^{-6}$ Torr and 400 V accelerating potential are shown. Even after a short exposure the crystal surface is extensively reduced. The corresponding tungsten states were found in the same curve-fitting procedure as before, using four tungsten 4*f* doublets, corresponding to $W^{6+}$, $W^{5+}$, $W^{4+}$, and $W^0$. The chemical shifts of $W^{4+}$ and $W^0$ were taken from Colton *et al.* (*24*). The distribution of valence states of tungsten under different reduction conditions are given in Fig. 8. Reduction of $WO_3$ to the metal via the formation of $WO_2$ has also been observed by Kim *et al.* (*25*).

The question arises as to what happens to Mo under weak $Ar^+$ bombardment. To answer this, $W_{0.53}Mo_{0.47}O_3$ was bombarded and examined by XPS after reduction. It was found that both W and Mo are reduced, the molybdenum being affected to a greater degree. This result is in accordance with the observations of Kim *et al.* (*25*) who demonstrated a correlation between the ease of reduction of oxides by $Ar^+$ bombardment and their standard free energy of formation. We expect therefore that oxygen ions associated with molybdenum positions in the structure will be more easily removed than those directly bound to tungsten.

## Discussion

### *The $W^{5+}$ and $Mo^{5+}$ Valence States*

In all reduced crystalline materials and coloured films studied by XPS the first

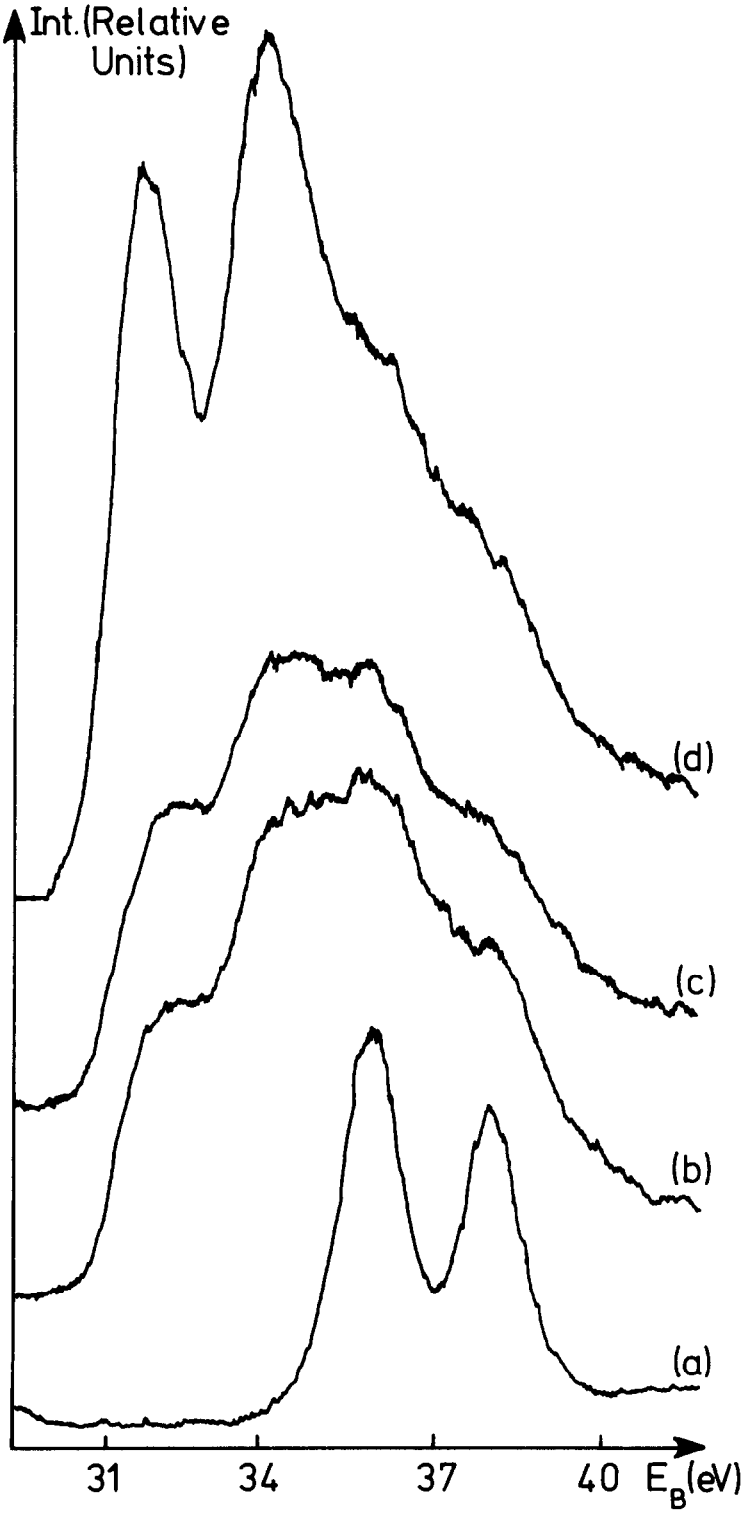


FIG. 7. W(4*f*) spectra from a $WO_3$ sample: (a) as-prepared crystals; (b) after argon ion bombardment (argon pressure = $3 \times 10^{-4}$ Torr, accelerating potential = 400 V, sample temperature = 300°K) for 30 min; (c) as for (b) but measured with a reduced electron take-off angle; (d) after bombardment for 150 min.

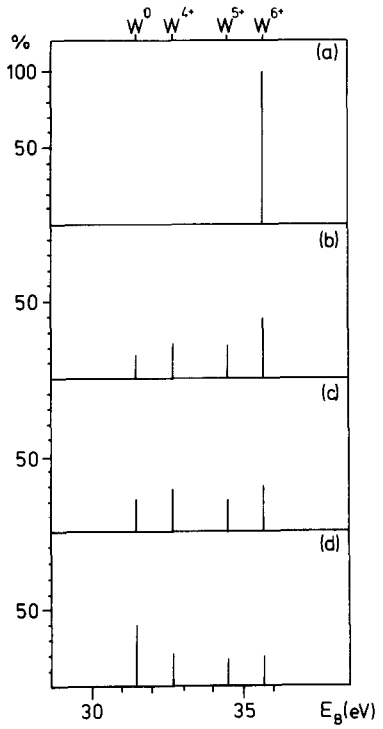


FIG. 8. Plot showing the distribution of tungsten valence states in a $WO_3$ sample after periods of argon ion bombardment. Conditions (a)–(d) as for Fig. 7.

reduced metal state is indexed as 5+ in accordance with the observed chemical shift. In the case of $W^{5+}$ the shift is ca. 1.2 eV below $W^{6+}$ (Table 1) and ca. 1.8 eV above $W^{4+}$. Though $W^{5+}$ seems to be the dominant reduced valence state in these materials, no nonmetallic compound with mostly five-valent ions of tungsten or molybdenum is known, although the surface of commercial $MoO_2$ has been shown to consist of $MoO_3$ and $MoO_x$ with $2 < x < 3$ (*25*). In pseudo-cubic metallic bronzes like $Na_xWO_3$ all tungsten states shift continuously because the induced-charge carriers are mostly delocalized (*26*), whereas, in low symmetric semiconducting $WO_3$-like sodium bronzes ($x < 0.28$), the charge carriers are trapped as $W^{5+}$ with a maximum ratio of $W^{5+}/W^{6+} = 0.39$. For higher degrees of reduction a structural phase transformation to the metallic bronzes takes place (*27*). This M–I transformation is therefore correlated with delocalization/localization effects and it is doubtful whether percolation models [e.g., ref. (*28*)] alone can describe this phase transition.

Together with the increase in the number of five-valent states, in all compounds studied the conductivity increases. This is reflected in the XPS data by a simultaneous increase of $M^{5+}$ and polaron states near the Fermi level (*24*). As this effect appears in *CS* phases as well as in bronzes, the occurrence of *CS* planes cannot be a necessary condition for $M^{5+}$ formation. Two correlations between $M^{5+}$ and quasifree charge carriers are possible: Both particles are connected in space or they are separated. Experimentally, Berak and Sienko (*9*) found, in slightly reduced tungsten oxide with Anderson–Hyde (*29*) finite shear planes, ca. 25% of the reduced states contributing to conductivity. These charge carriers must be localized between *CS* disks because no macroscopic conductivity can occur from these highly diluted states according to percolation theory. Since the creation of $W^{5+}$ is not restricted to *CS* planes and can occur to some extent between them, they are likely to be induced by weakly bound electrons which form together with the surrounding distorted lattice polarons of different size (*8, 9*).

The two possible metal positions, W and Mo, show different reduction behavior in the mixed crystals. According to Table I ca. 20% Mo, but only 1.3% W, appears in the five-valent state. The nominal chemical composition of the reduced mixed crystal is therefore $Mo^{5+}_{0.03}Mo^{6+}_{0.17}W^{5+}_{0.01}W^{6+}_{0.8}O_{2.94}$. Due to the fact that in metal-reduced samples most reduced states are localized in the *CS* planes (*13b*) it is expected that Mo is enriched in the *CS* planes. It is even possible that in the equilibrium state all central positions of edge-sharing octahedra are occupied by Mo. Additional $W^{5+}$ states may appear between *CS* planes. This preferential occupancy of Mo in closer packed octahedral positions

resembles the pure $MoO_3$ structure with a short metal-metal distance of 2.6 Å.

In addition to structural effects, the preferential reduction of Mo is explained by the slightly lower trapping energy of Mo compared with W. According to Faughnan and Crandall (*30*) the energy difference in amorphous material is 0.73 eV. We hope to pursue this question by optical experiments and X-ray structure analysis of reduced single crystals.

*The Effect of Crystallinity*

All core-level spectra of the examined material show a characteristic dependence of the 4*f* levels on the crystallinity of the sample. In all reduced single crystals only $W^{6+}$ and $W^{5+}$ valence states dominate the XPS spectra. On the other hand, after strong $Ar^+$ bombardment of the single crystals the surface region showed considerable $W^{4+}$ and $W^0$ signals. Since under bombardment oxygen is preferentially removed from the surface, the crystallinity is destroyed and closer packing of the metal positions in a glass is expected, leading even to the formation of metallic clusters. This observation is in accordance with experiments of Gerard *et al.* (*31*), who found similar spectra in amorphous $WO_{3-x}(x = 0.2 \ldots 0.5)$. A comparison of their results with the distribution of the reduced tungsten states in Fig. 8 show that our highest reduced noncrystalline material corresponds to amorphous $WO_{1.4}$. In colored films at least the electron charges are strongly localized forming all reduced tungsten states. As Schirmer *et al.* (*10*) pointed out this localization of electrons as small polarons is much stronger in amorphous films than in crystalline material and represents the basis of the application of $WO_3$ in electrochromic devices. Whereas in crystals surplus charges are only slightly trapped under formation of $W^{5+}$ states the amorphous colored state exhibits stronger localization in different reduced tungsten valence states, probably depending on the local crystal field at the tungsten site and hence depending on the preparation method of the tungsten oxide glass.

Spectra similar to those of amorphous material (e.g., thin films) have recently been published by Haber *et al.* (*13*) and Haber (*32*). In the $WO_3$ material used by them, highly reduced tungsten valence states occur after much weaker $H^+$ bombardments than used in our experiments. Both studies were performed with identical photoelectron spectrometers and under similar conditions so that the explanation for the different results must be due to different sample material. These authors used very fine-grained quasiamorphous $WO_3$ (as is commercially available) and not as-grown crystals. Furthermore, they found no reduction of tungsten oxide by heating *in vacuo* at 500°C, which is a widely used technique to produce slightly surface-reduced tungsten oxide. Control experiments on our single crystals showed the appearance of $W^{5+}$ states at the surface even after heating the specimens for 6 hr at 250°C *in vacuo*. The term "amorphous" does not necessarily mean that these substances do not show X-ray reflections. As Anderson (*33*) found, even $WO_3$ ceramic, although fairly X-ray crystalline, behaves differently from single crystals in showing no thermal structural phase transformations. Great care must therefore be taken in producing crystalline tungsten oxide, even for the examination of short-range effects as in XPS experiments. Besides the already described differences in the photoelectron spectra between crystalline and amorphous materials, smaller effects are expected due to structural phase transformations as seen in similar compounds by Thornton *et al.* (*34, 35*).

*The Structural Transformation $\varepsilon$–$\delta$*

During cooling, slightly reduced $WO_3(H^+$ in $WO_3)$ shows the phase transformation $\varepsilon$–$\delta$ (*36*) in X-ray experiments. Our XPS data for

a weakly $H^+$-bombarded crystal indicate that, simultaneously, the linewidth of the W(4*f*) peak characteristic of the five-valent tungsten position changes from 1.5 to 1.1 eV, but no change occurs in the six-valent tungsten signal (Fig. 5 and Table I). This phase transition is of the metal–insulator type, similar to that of $VO_2$. In vanadium oxide a corresponding broadening of vanadium lines was observed by Blaaw *et al.* (*16b*). Following their interpretation of general linewidth effects, two different limiting cases must be distinguished:

(a) The energy of the core hole–valence electron interaction $U$ is small compared with the gap energy $E_g$. No irregular broadening is expected in this case.

(b) If $U$ is large compared with $E_g$ an asymmetric broadened line shape is expected as for metallic materials. Further broadening will occur if not only the gap energy $E_g$ but also the valence bandwidth $E$ is small or comparable with $U$. Both limiting cases seem to apply to doped $WO_3$:$H^+$. The intrinsic band gap is 2.74 eV at room temperature and 3.2 eV at low temperature. Both values are large compared with typical core hole–valence electron interactions and therefore no broadening of the intrinsic $W^{6+}$ states is expected during the phase transformation.

The five-valent tungsten states show hopping activation energies of 0.23 eV in the low-temperature phase and of almost zero at room temperature (*9*). Furthermore, these states are rather localized, so that when treated as small polaron bands with Anderson localization, their bandwidth is negligible compared with $U$. Both conditions for line broadening are therefore fulfilled and a spontaneous change in the linewidth of $W^{5+}$ is expected when passing through the phase-transition point.

There are, however, additional line-broadening effects at high temperatures. Firstly, phonon-broadening effects are possible for $W^{5+}$. The five-valent tungsten state is localized by electron–phonon coupling and hence by a considerable lattice deformation near the $W^{5+}$ position. The drastic change in the crystal structure during the phase transformation alters the deformation behavior and changes in the phonon broadening may contribute to the observed difference in the $W^{5+}$ half-width of 0.4 eV.

Furthermore, only in the low-temperature phase do the electrons trapped at $W^{5+}$ form oriented $d(x^2-y^2)$ orbitals. As Schirmer *et al.* (*10*) found by ESR measurements, all these $d$ orbitals lie in the $a$–$b$ plane, but are randomly orientated at higher temperatures. In our single-crystal work, the crystal surface was always (001). We would expect photoemission from the oriented orbitals to exhibit a strong angular dependence. Averaging over all directions for $W^{6+}$ and $W^{5+}$ at room temperature then gives rise simply to spectral line broadening whereas at low temperature a narrower $W^{5+}$ line is expected. Hence angular resolved XPS experiments on doped $\varepsilon$-$WO_3$ should show different $W^{5+}$ signals perpendicular and parallel to the crystallographic $c$ axis. These experiments are planned. Additional final-state effects were very recently proposed by Chalzalviel *et al.* (*37*) and Wertheim *et al.* (*38*) to explain the splitting of W-4*f* core levels in metallic sodium bronzes. In the case of slightly reduced tungsten oxide, this effect is expected to be comparably small. Nevertheless, it should be examined whether these models can explain the observed temperature dependence of the linewidth of the $W^{5+}$ signal (Fig. 5, Table 1).

## Acknowledgments

We acknowledge the Science Research Council for their general support. One of us (E.S.) was a guest scientist under the aegis of the Royal Society European Exchange Scheme.

## References

1. N. F. MOTT, *Proc. Phys. Soc. A* **62**, 416 (1949).
2. N. F. MOTT, *Rev. Mod. Phys.* **40**, 677 (1968).

3. R. W. JOYNER, K. KISHI, AND M. W. ROBERTS, *Proc. Roy. Soc. London A* **358**, 223 (1977); M. W. ROBERTS, *Chem. Soc. Rev.* **6**, 373 (1977).
4. A. F. CARLEY AND M. W. ROBERTS, *Proc. Roy. Soc. London A* **363**, 403 (1978).
5. S. K. DEB, *Phil. Mag.* **27**, 801 (1973).
6. M. R. TUBBS, *Phys. Status Solidi A* **21**, 253 (1974).
7. E. SALJE, R. GEHLIG, AND K. VISWANATHAN, *J. Solid State Chem.* **25**, 239 (1978).
8. E. SALJE, *Opt. Commun.* **24**, 231 (1978).
9. J. M. BERAK AND M. J. SIENKO, *J. Solid State Chem.* **2**, 109 (1970).
10. O. F. SCHIRMER, V. WITTWER, W. BAUR, AND G. BRANDT, *J. Electrochem. Soc.* **24**, 749 (1977).
11. G. HOPPMANN AND E. SALJE, *J. Phys. Status Solidi A* **37**, K187 (1976).
12. G. HOLLINGER, TRAN MINH DUC, AND A. DENEUVILLE, *Phys. Rev. Lett.* **37**, 1564 (1976).
13. (*a*) J. HABER, J. STOCH, AND L. UNGIER, *J. Solid State Chem.* **19**, 113 (1976). (*b*) B. A. DEANGELIS AND M. SCHIAVELLO, *J. Solid State Chem.* **21**, 67 (1977).
14. K. SIEGBAHN, G. NORDLING, A. FAHLMAN, R. NORDBERG, K. HAMRIN, J. HEDMAN, G. JOHANSSON, T. BERGMARK, S. E. KARLSSON, I. LINDGREN, AND B. LINDBERG, "ESCA—Atomic, Molecular and Solid State Structure Studied by means of Photoelectron Spectroscopy," Almqvist & Wiksells, Stockholm (1967).
15. R. W. JOYNER, *Surface Sci.* **63**, 291 (1977).
16. (*a*) S. DONIACH AND M. SUNJIC, *J. Phys. C* **3**, 285 (1970); (*b*) C. BLAAW, F. LEENHOUTS, F.V.D. WOUDE, AND G. A. SAWATZKY, *J. Phys. C* **8**, 459 (1975).
17. (*a*) C. R. BRUNDLE, M. W. ROBERTS, D. LATHAM, AND K. YATES, *J. Electron Spectrosc.* **3**, 241 (1974); (*b*) M. J. BRAITHWAITE, R. W. JOYNER, AND M. W. ROBERTS, *Faraday Discuss. Chem. Soc.* **60**, 89 (1975).
18. S. EVANS, *in* "Handbook of X-ray and Ultra-violet Photoelectron Spectroscopy" (D. Briggs, Ed.), pp. 121–151, Heyden and Son, London (1977).
19. E. SALJE AND K. VISWANATHAN, *Acta Crystallogr. A* **31**, 356 (1975).
20. T. ENGSTROEM, E. SALJE, AND R. J. D. TILLEY, *J. Solid State Chem.*, submitted.
21. R. D. FRASER AND E. SUZUKI, *in* "Spectral Analysis" (J. A. Blackburn, Ed.), pp. 171–211, Dekker, New York (1970).
22. J. A. TOSSEL, *J. Electron Spectrosc.* **8**, 1 (1976).
23. D. E. EASTMAN, *Phys. Rev. Lett.* **34**, 395 (1975).
24. R. J. COLTON, J. W. RABALAIS, AND A. M. GUZMAN, *Accounts Chem. Res.*, in press.
25. K. S. KIM, W. E. BAITINGER, J. W. AMY, AND N. WINOGRAD, *J. Electron Spectrosc.* **5**, 351 (1975).
26. M. CAMPAGNA, G. K. WERTHEIM, H. R. SHANKS, F. ZUMSTEG, AND E. BANKS, *Phys. Rev. Lett.* **34**, 738 (1975).
27. E. SALJE, *Ferroelectrics* **12**, 215 (1976).
28. I. WEBMAN, J. JORTNER, AND M. H. COHEN, *Phys. Rev. B* **13**, 713 (1976).
29. J. S. ANDERSON AND B. G. HYDE, *J. Phys. Chem. Solids* **28**, 1393 (1967).
30. B. W. FAUGHNAN AND R. S. CRANDALL, *Appl. Phys. Lett.* **31**, 834 (1977).
31. P. GERARD, A. DENEUVILLE, G. HOLLINGER, AND TRAN MINH DUC, *J. Appl. Phys.* **48**, 4252 (1977).
32. J. HABER, *J. Less-Common Metals* **54**, 243 (1977).
33. A. ANDERSON, *Spectrosc. Lett.* **9**, 809 (1976).
34. G. THORNTON, A. F. ORCHARD, AND C. N. R. RAO, *Phys. Lett. A* **54**, 235 (1975).
35. G. THORNTON, A. F. ORCHARD, AND C. N. RAO, *J. Phys. C* **9**, 1991 (1976).
36. G. HOPPMANN, to be published.
37. J. N. CHAZALVIEL, M. CAMPAGNA, G. K. WERTHEIM, AND H. R. SHANKS, *Phys. Rev. B* **16**, 697 (1977).
38. G. K. WERTHEIM, M. CAMPAGNA, J. N. CHAZALVIEL, D. N. E. BUCHANAN, AND H. R. SHANKS, *Appl. Phys. (Germany)* **13**, 225 (1977).